Heliyon 9 (2023) e20503

Contents lists available at ScienceDirect

Heliyon

journal homepage: www.cell.com/heliyon

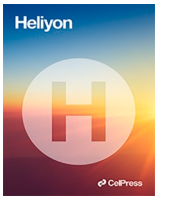

Characterization of texturized meat analogues containing native lupin flour and lupin protein concentrate/isolate

J.M. Ramos-Diaz [a,c,*], S. Oksanen [a], K. Kantanen [a], J.M. Edelmann [a], H. Suhonen [b], T. Sontag-Strohm [a], V. Piironen [a], K. Jouppila [a]

[a] Department of Food and Nutrition, University of Helsinki, Agnes Sjöbergin katu 2, FI-00014, Helsinki, Finland
[b] Department of Physics, University of Helsinki, Gustaf Hällströmin katu 2, FI-00014, Helsinki, Finland
[c] Natural Resources Institute Finland, Myllytie 1, FI-31600, Jokioinen, Finland

ARTICLE INFO

Keywords:
High moisture extrusion
Meat analogues
Lupin
Protein concentrate
Protein isolate

ABSTRACT

Lupin is a nutritious, yet undervalued grain used as a fodder and food crop. In the present study, native lupin flour (LF), lupin protein concentrate (LPC), and lupin protein isolate (LPI) were combined (70% LPI:LPC blend ratios [30:70, 50:50, and 70:30] and 30% LF constant fraction), extruded at high moisture (45–55%), and shaped with a long cooling die (800 mm) to obtain texturized meat analogues (TMAs) with fibrous structures. The characteristics of TMAs (e.g., hardness, water hydration capacity) depended heavily on water content, blend ratios (LPI:LPC), and to a lesser extent, the long cooling die temperature. Color changes (i.e., L*, b*) were mostly attributed to variations in blend ratios (LPI:LPC). Microstructure analysis showed that TMAs with higher water content (55%) were more likely to have thinner walls and smaller void thickness. Fluorescence imagery revealed that TMAs with lower LPI content presented more homogeneous structures. These findings show that reasonable amounts (30% d.m.) of native lupin flour can be incorporated into meat analogues by maintaining a sufficiently high protein content (>50% d.m.) to trigger the formation of fibrous structures.

1. Introduction

The consumption of plant-based meat analogues is increasing in the developed world. This responds to (i) growing public awareness of the carbon footprint associated with the meat industry, (ii) stronger attitudes toward health promotion (e.g., cardiovascular diseases, obesity, type II diabetes), and (iii) current ethical constraint due to animal welfare [1,2]. Despite efforts to develop plant-based alternatives to meat, the reliance on a handful of imported feed grains (e.g., wheat, corn, soybean) imposes new challenges that could be as environmentally detrimental as meat itself. Thus, the use of local grains could dramatically reduce the carbon footprint linked to transportation, secure the preservation of local varieties, prevent the introduction of foreign species to vulnerable ecosystems, revalue/foster domestic culinary knowledge, and boost food system resilience [3,4]. In this context, blue lupin (*Lupinus angustifolius*) is a plant whose seeds (hereafter referred to as *lupin*) are rich sources of protein (31–40%) and dietary fiber (15–25%) [5–8]. Although traditionally used as animal feed, a reassessment of lupin's nutritional and technological characteristics could increase its human consumption and valorization worldwide.

Most of lupin's protein fraction is made of four types of globulins: α-, β-, γ- and δ-conglutin (11S, 7S, 7S, and 2S, respectively). α- and

* Corresponding author. P.O. Box 66 (Agnes Sjöbergin katu 2), University of Helsinki, FI-00014, Finland.
E-mail address: jose.ramosdiaz@helsinki.fi (J.M. Ramos-Diaz).

https://doi.org/10.1016/j.heliyon.2023.e20503
Received 4 July 2023; Received in revised form 11 September 2023; Accepted 27 September 2023
Available online 5 October 2023

Abbreviations

AI	anisotropy index
D-WHC	Water hydration capacity measured via destructive method
TMAs	Texturized meat analogues
LCDT	Long cooling die temperature
MLR	Multiple Linear Regression Analysis
ND-OAC	Oil absorption capacity measured via non-destructive method
ND-WHC	Water hydration capacity measured via non-destructive method
LF	Lupin flour
LPC	Lupin protein concentrate
LPI	Lupin protein isolate
PLSR	Partial Least Squares Regression Analysis
Ten	Tensile cutting strength
Tran	Transverse cutting strength
WAI	Water absorption index
WSI	Water solubility index

β-conglutin make up most of total globulin, while the presence of γ- and δ-conglutin is comparatively small [9]. Even though the overall protein content of native lupin might depend on the cultivated species/varieties, tillage system, harvesting season, and rainfall environment [10,11], researchers [12–14] have observed that lupin has (on average) a similar content of protein and higher content of dietary fiber than soybean (*Glycine max*). Similarly, lupin was found to have a higher content of protein and dietary fiber and a lower content of carbohydrates than pea (*Pisum sativum*) [13]. This gives lupin the potential to substitute soybeans and peas.

In its native form, lupin presents substantial contents (≥50% d.m.) of non-starch polysaccharides (NSPs), such as galactomannans, glucomannans, mannans, and galactans [15,16]. Based on Fourier-transform infrared spectroscopy, β-glycoside linkages (877.9 cm^{-1}), pyranose rings (989.5 cm^{-1}; 1067.5 cm^{-1}; 1103.3 cm^{-1}) and carbonyl bonds (as part of an amide group; 1539.4 cm^{-1}) were detected in NSPs extracted from blue lupin [15]. These NSPs contained mostly (in decreasing order) galactose, mannose, xylose, rhamnose, glucose, and fucose.

Compared to other grains, there are few studies on the nutritional benefits of lupin. Among these [17,18], demonstrated the probiotic activities of NSPs extracted from lupin. For instance, a diet rich in NSPs seems to stimulate the growth of bifidobacteria (*Bifidobacterium* spp.), thus altering the composition of the colonic microbiota in healthy men [17]. Lupin also contains notable amounts of phenolic compounds (total phenolics: 13.0 mg/g, flavonoids: 4.4 mg/g, flavonols: 1.7 mg/g; average values reported by Ref. [19], B vitamins (vitamin B1 [thiamine]: 7.1 mg/kg, vitamin B2 [riboflavin]: 2.4 mg/kg; [20], tocopherols (alpha-T: 0.4 mg/100 g, gamma-T: 8.0 mg/100 g, total T: 8.4 mg/100 g; average values calculated from data reported by Ref. [21], and carotenoids (total carotenoids: 229 μg/g, lutein: 24.1 μg/g, zeaxanthin: 134.4 μg/g, beta-carotene: around 50 μg/g; [22].

Technologically, considerable advances have been made to understand the role of lupin flour in wheat-based popular food products, such as bread, gluten-free cakes, instant noodles, and pasta (Martinez-Villaluenga et al., 2010 [23,24]; Levent et al., 2011). According to Ref. [25]; adding only 10% lupin flour to refined wheat flour-based bread resulted in an observable detrimental quality. This is usually connected to the low elasticity associated with proteins and the high water-binding capacity of dietary fiber in lupin. The few studies found on lupin-containing meat analogues use mostly protein concentrates and isolates [26,27], raw materials—particularly isolates—that require substantial amounts of energy and water for their production. According to Ref. [26]; it is possible to obtain meat-mimicking fibrous structures from a blend of lupin protein concentrate and isolate (50:50) at 55% water content, with the most influential factor being water content compared to barrel temperature and screw speed.

In general, high moisture extrusion coupled with a long cooling die should offer the conditions for protein-rich materials to undergo phase separation and aggregation, and potentially result in the formation of layered and oriented fibrous structures. However, a myriad of intrinsic factors may influence the outcome, including (i) the ratio of non-proteinaceous components, (ii) pH value, (iii) ions, and (iv) emulsifying properties, among others [28].

The present investigation aimed to set a benchmark for the development of meat analogues containing native lupin flour. Physical/physicochemical characteristics of extruded meat analogues containing native lupin flour and protein ingredients (blends of protein concentrate and isolate) were measured, analyzed, and modelled following regression analyses (multiple linear regression [MLR] and partial least squares regression [PLSR]). This study introduced native lupin flour (around 1/3) to meat analogues to boost health benefits and reduce reliance on high resource-consuming protein ingredients.

2. Material and methods

2.1. Materials

Lupin flour (LF; FRANK Food Products, Twello, Netherlands), lupin protein concentrate (LPC; FRANK Food Products, Twello, Netherlands), and lupin protein isolate (LPI; Prolupin GmbH, Grimmen, Germany) were purchased and stored in frozen storage

(−20 °C) prior to blending. Three mixtures containing a constant fraction of LF (30% d.m.) and a blend of protein ingredients (70% d.m. [LPI:LPC; 30:70, 50:50, and 70:30]) were prepared for testing (Table 1). Protein content analysis followed the Dumas combustion method (Vario MAX CN, Germany) using a nitrogen-to-protein conversion factor of 5.4. The contents of fat, dietary fiber, and carbohydrate were analyzed and provided by the manufacturer (Table 1). The water absorption index (WAI) and water solubility index (WSI) of each ingredient (LF, LPC, and LPI) were measured following the method reported by Ref. [29]; deionized water was used as the solvent. The particle diameter (of powder granules) was measured using a laser diffraction particle size analyzer (Mastersizer 3000 SM, Malvern Instruments Ltd., Worcestershire, UK) with a dry powder dispersion unit (Aero S). The refractive index was set at 1.46. Chemical and physicochemical analyses were conducted in triplicate.

2.2. Extrusion process

Texturized meat analogues (TMAs) were prepared at different LPI:LPC blend ratios (70% blend [LPI:LPC; 30:70, 50:50, and 70:30] and 30% LF), water contents (WC: 45, 50, and 55%) and long cooling die temperatures (LCDT: 40, 60, and 80 °C). This was done following a split-plot Box-Behnken experimental design (Appendix A). A twin-screw laboratory extruder (Thermo Prism PTW24 Thermo Haake, Polylab System, Germany) attached to a long cooling die (flat cooling nozzle FKD75, DIL Deutsches Institut für Lebensmitteltechnik, Quakenbrück, Germany) was used to produce the TMAs. Reverse osmosis water was the only liquid ingredient fed into the extruder, and the total feed rate and screw speed were maintained at 50 g/min and 400 rpm, respectively. The technical details of the equipment are shown in Appendix B. At the exit point, the TMAs were cut into pieces of 20 cm in length and placed inside Ziplock bags for subsequent storage at −20 °C.

2.3. Determination of mechanical and physicochemical properties

The properties of the TMAs were assessed with a Texture Analyzer TAXT2i (Stable Micro Systems, Surrey, England). For the *texture profile analysis* (TPA), TMAs were cut into cubical specimens [24 mm (W) × 24 mm (L) × 14 mm (H)] and placed on a flat square aluminum sample holder. A cylindrical probe (Ø 36 mm) was fixed to a mechanical arm, and performed two sequential vertical descents on every specimen, while force-time data was registered. The settings of the probe were as follows: load cell, 50 kg; pre-test speed, 1 mm/s; test speed, 1 mm/s; post-test speed, 5 mm/s; deformation distance, 7 mm (50% strain); resting time, 5 s; and trigger force, 5 g. Each measurement resulted in a two-cycle force-time curve from which hardness, springiness, and chewiness were calculated using Equations (1)–(3), respectively.

$$\text{Hardness} = F_{\max \rightarrow A_1} \tag{1}$$

$$\text{Springiness} = \frac{L_2}{L_1} \tag{2}$$

$$\text{Chewiness} = \frac{A_2}{A_1} \times \text{Hardness} \times \text{Springiness} \tag{3}$$

where, A_1 or A_2 is the area (N.s) to the peak force corresponding to cycle 1 or cycle 2, respectively; $F_{\max \rightarrow A_1}$ is the maximum force (N) corresponding to area A_1; L_1 or L_2 is the period (s) corresponding to A_1 or A_2, respectively. To assess the *cutting strength*, TMAs were cut

Table 1
Chemical, physical and physicochemical characterization of individual raw materials (lupin flour, *LF*; lupin protein concentrate, *LPC*; lupin protein isolate, *LPI*) and their mixtures. Water absorption index, *WAI*; water solubility index, *WSI*; surface area moment mean, *D[3,2]*; volume moment mean, *D[4,3]*.

	LF, %	LPC, %	LPI, %	Blend ratios	Content (g/100 g d m.)				WAI	WSI	D [3,2]	D [4,3]
				[a]LPI:LPC	Protein	[b]Fat	[b]Dietary fibre	[b]CHO				
LF	100	–	–	–	36.8 ± 0.3	7.9	36	7.5	267.8 ± 1.2	20.2 ± 0.2	22.9 ± 0.1	54.1 ± 0.3
LPC	–	100	–	0:100	54.6 ± 0.1	9.8	14.6	7.6	191.5 ± 1.5	24.2 ± 1.1	9.9 ± 0.1	12.9 ± 0.3
LPI	–	–	100	100:0	97.5 ± 0.0	3.0	4.4	0.5	244.2 ± 6.9	56.3 ± 1.3	49.9 ± 0.5	77.3 ± 0.9
Mixture 1 (M1)	30	49	21	30:70	58.2	7.8	18.9	6.1	211.7 ± 0.9	35.9 ± 0.5	16.6 ± 0.1	46.7 ± 0.2
Mixture 2 (M2)	30	35	35	50:50	64.2	6.9	17.5	5.1	234.4 ± 3.9	45.5 ± 4.1	20.5 ± 0.1	56.2 ± 0.5
Mixture 3 (M3)	30	21	49	70:30	70.3	5.9	16.0	4.1	229.0 ± 1.9	48.5 ± 0.2	26.4 ± 0.1	64.2 ± 0.2

[a] Blend ratios (LPI:LPC) 30:70, 50:50 and 70:30 correspond to mixtures 1, 2 and 3 (M1-M3), respectively.
[b] Data provided by producer.

into pieces of specific dimensions [20 mm (W) × 30 mm (L) × 10 mm (H)] and tested following two cutting directions: transverse (*defn.* perpendicular to the flow direction) and tensile (*defn.* flow direction) (Appendix C). A probe attached to a razor blade performed a cut upon descent using the following settings: load cell, 5 kg; pre-test speed, 1 mm/s; test speed, 1 mm/s; post-test speed, 5 mm/s; and cutting distance, 10 mm. The collected data were the maximum force (N). The *anisotropy index* (AI) was calculated as the ratio between transverse and tensile ($\frac{transverse}{tensile}$) cutting strength (Appendix A).

To measure the *destructive water hydration capacity* (D-WHC), TMAs were shredded and then dried in an airflow convection oven (Termaks, Bergen, Norway) at 50 °C for 12 h. Dried samples were milled with an ultra-centrifugal mill (Retsch ZM 200, Haan, Germany; rotational speed, 10,000 rpm) and stored in Ziplock bags at room temperature (25 °C) prior to analysis [30]. To assess the *non-destructive water hydration/oil absorption capacity* (ND-WHC; ND-OAC), TMAs were cut into pieces of the following dimensions: 2 cm × 3 cm × 1 cm, and dried in an airflow convection oven (Termaks, Bergen, Norway) at 40 °C for about 24 h. Each piece was weighed and placed in a 50-ml Eppendorf tube, and then immersed in 40 ml of Milli Q water or rapeseed oil (Keiju, Bunge Finland Ltd., Finland) at 50 °C (water bath) for 16 h, followed by draining for 5 min. ND-WHC or ND-OAC were expressed as grams of water/oil retained per gram of dried sample using Equation (4),

$$ND\text{-}WHC\ or\ ND\text{-}OAC(\%) = \frac{(W_{AR} - W_{BR})}{W_{BR}} \times 100 \tag{4}$$

where W_{AR} is the weight of the sample after rehydration/oil absorption and W_{BR} is the weight of the sample before rehydration/oil absorption.

The color space parameters lightness (L*), redness (a*), and yellowness(b*) were measure using a Minolta CR-400 chromometer (Konica Minolta Sensing, Inc., Osaka, Japan) on the exposed inner side (upon cut-opening) of defrosted TMAs; frozen samples were placed inside a Ziplock bag and exposed to water bath heating for 1 h at 30 °C.

2.4. Imaging analyses

TMAs were cut into pieces of defined volume (Appendix C, transverse) and freeze-dried (Lyovac GT 2, Amsco Finn-Aqua GmbH, Hürth, Germany) for 4 days. Images of freeze-dried TMAs were obtained via X-ray micro-CT system phoenix nanotom|s (phoenix|x-ray Systems + Services GmbH, currently part of Waygate Technologies owned by Baker Hughes). The samples were placed in a small plastic cup and supported by Styrofoam balls to ensure immobility during the scan. The operating voltage was 60 kV and the current 150 μA; no filter was used. Each sample was imaged by taking 1600 projection images around 360° rotation with an exposure time of 3 × 500 ms per projection. The pixel size of the images was 20 μm. 3D volumes were generated using phoenix datos|x 2 reconstruction software version 2.4.0 (phoenix|x-ray Systems + Services GmbH). The image analysis was conducted in Fiji/ImageJ [31,32]. Noise reduction was done by non-local means denoising [33,34], and the void portion was then identified by choosing (manually) a threshold value (the same for all samples) below which gray scale values were considered void space. The thickness distribution for the void space was computed using the ImageJ LocalThickness plugin [35].

The compositional and structural characteristics of TMAs were observed using an Axio Scope A1 fluorescence microscope (Carl Zeiss Microscopy GmbH, Germany) connected with an AxioCam 305 color digital camera (Carl Zeiss, Microimaging GmbH, Göttingen, Germany) and equipped with an external fluorescence light source (HXP 120 V, Carl Zeiss, Germany). Flat rectangular pieces (20 mm × 28 mm × 1 mm), taken from the center and side, were cut out from selected TMAs and submerged in Nile Blue A (Sigma-Aldrich) solution (0.1% w/v) for 15 min. The resulting samples were placed individually in perforated case holders and rinsed with Milli-Q water. Excess water was removed from the surface of the sample by using a vacuum oven (ThermoStable OV-70, Daihan Scientific Co. Ltd, Wonju-si, Korea) at 40 °C for 30 min. The samples were placed between two glass slides and taped to each other to keep the sample flat and steady during image acquisition. The excitation and emission wavelengths of Nile Blue A for the detection of proteins were 635 and 674 nm, respectively (red channel detector). Color interpretation took place as follows: black, soluble/insoluble dietary fiber and carbohydrates; red, native/denatured protein; white, spectral overlap associated to the presence of neutral lipids (e.g., triglycerides). Photographs were taken using Zen 3.2 Blue edition (Carl Zeiss Microscopy GmbH, Germany) and eventually stitched using an Image Composite Editor (ICE, Microsoft corporation) for the observation of macrostructures. Ten individual pictures—corresponding to each tested sample—were stitched together for analysis. Images were subsequently analyzed in Fiji/ImageJ software. The color difference between the side and the center of the TMAs was calculated using a modified version of the delta E (ΔmE) formula:

$$\Delta mE = \sqrt{\Delta Mean^2 + 2(\Delta Mode)} \tag{5}$$

where Δ *Mean* is the numerical difference between the mean values of the red color histogram and Δ *Mode* is the absolute difference between the mode values of the red color histogram.

Photographs of selected TMAs (thawed, cut into 5-cm pieces, and split open) were taken with a digital single-lens reflex (DSLR) body camera (Nikon 7200, Tokyo, Japan) attached to a telephoto lens (18–400 mm f/3.5–6.3 DI II VC HLD zoom objective, Tamron Co., Ltd., Saitama, Japan) in a light-controlled cabinet (D50, warm daylight). The settings were as follows: distance to object, 20 cm; magnification, 18 mm; aperture, 9; shutter speed, 250; and ISO, 1000. Raw images (NEF format) were processed with Corel PaintShop Pro (v. 2021, Corel Corporation, Ottawa, Canada).

Table 2
Effects of independent variables (blend ratio between lupin protein isolate and concentrate, *LPI:LPC*; water content, *WC*; long cooling die temperature, *LCDT*) on physicochemical and mechanical properties of meat analogues. Torque, *Tor*; pressure, *Pre*; hardness, *Hard*; chewiness, *Chew*; springiness, *Spring*; water hydration capacity, *WHC*; oil absorption capacity, *OAC*; tensile cutting strength, *Ten*; transverse cutting strength, *Tran*; lightness, *L**; redness, *a**; yellowness, *b**.

	Tor	Pre	Hard	Chew	Spring[a]	Non-destructive		Destructive	Cutting strength		L*	a*[a]	b*
						WHC[a b]	OAC[a]	WHC	Ten	Tran			
Constant	15.3	5.5	347.6	172.6	0.87	96.7	4.4	1.9	12.3	10.7	42.1	4.2	19.0
L = LPI:LPC[c]	0.91**	0.12	24.0*	27.2**	0.02	2.5	−1.3	0.06***	0.12	0.56	−3.2***	−0.01	−1.9***
W = WC	−3.4***	−1.49***	−154.0***	−78.0***	0.006	10.9	0.01	0.13***	−6.7***	−4.1***	3.1***	0.07	1.9***
T = LCDT	−0.25	−0.58*	15.3	9.3	−0.01	−3.4	0.04	−0.03*	1.7**	0.09	−1.1**	−0.08	−0.50
*L*L*	−0.50	−0.002	1.8	−3.5	−0.04	−5.7	−0.34	−0.05*	0.83	−0.09	2.0**	−0.24	0.89*
*W*W*	0.02	0.37	−1.6	−11.0	−0.002	10.6	1.8	0.06**	0.04	−1.4	1.1*	−0.22	0.32
*T*T*	0.23	−0.05	−4.4	0.46	0.02	3.2	0.55	−0.03	−0.09	0.54	0.07	0.25	0.16
*L*W*	−0.63	−0.22	−13.8	−7.7	0.020	3.3	−1.6	0.03	0.51	0.63	−1.4**	0.00	−0.92*
*L*T*	−0.12	−0.77*	−2.6	−5.4	−0.02	3.1	0.37	0.02	−0.97	0.12	0.17	0.13	0.26
*W*T*	0.24	0.73*	5.4	−2.10	−0.03	−3.4	−0.79	0.02	−0.57	−0.40	−1*	−0.25	−0.62
R2	0.96	0.93	0.98	0.96	0.60	0.53	0.40	0.97	0.97	0.93	0.98	0.51	0.97
Q2	0.66	0.37	0.75	0.56	−3.4	−3.5	−5.1	0.89	0.86	0.12	0.82	−4.2	0.75

*, **, *** Significant at $p < 0.05$, $p < 0.01$ and $p < 0.001$.
[a] Regression is NOT significant at level p of 5%.
[b] Lack of fit is significant at level p of 5%.
[c] 70% mixture (LPI:LPC; 30:70; 50:50; 70:30) + 30% LF.

2.5. Statistical analysis

The main effect of LPI:LPC blend ratios (70% blend [LPI:LPC; 30:70, 50:50, and 70:30] and 30% LF of solids), WC (45, 50, and 55%) and LCDT (40, 60, and 80 °C), and their corresponding squared effects and interactions on the mechanical/physicochemical properties of the TMAs were statistically analyzed via MLR analysis (MODDE v. 12.1, Umetrics, Sweden) and PLSR modeling (SIMCA v. 15.0, Umetrics, Sweden). PLSR coefficients and indicators of model suitability (root mean square error of cross validation, RMSEcv; coefficient of determination, R^2; coefficient of prediction, Q^2; variable importance in projection, VIP) are detailed in Appendix D. The complete dataset corresponding to every individual trial (17) is presented in Appendix A. TMAs measurements (e.g., TPA, WAI, WSI) were conducted at least in triplicate.

3. Results and discussion

3.1. Characterization of raw materials

The chemical composition and physicochemical characteristics of single ingredients (LF, LPC, and LPI) and mixtures (M1, M2, and M3) are detailed in Table 1. The protein content was evidently higher in LPI than in LPC and LF (LPC > LF). The contents of fat and dietary fiber were, however, the lowest in LPI. Less than 10% carbohydrates (CHO) were found in LF and LPC, and traces in LPI. The gradual decrease in macro components (i.e., fat, dietary fiber, CHO) among single ingredients was attributed to the protein separation process. Upon blending, disparities in the content of macro components reduced considerably. Even though M1 (30 LPI: 70 LPC) and M3 (70 LPI: 30 LPC) presented opposite blend ratios, the difference, in terms of protein content, was less than 10%, whereas the difference corresponding to fat, dietary fiber and CHO was less than 5%.

The lowest WAI value was found in LPC while the highest in LF. The protein content of single ingredients (LF < LPC < LPI) showed weak correlation with the corresponding WAI (LPC < LPI < LF). By contrast, the mixtures with higher protein content (M3 > M2 > M1) presented higher WAI (M2 = M3 > M1). The WSI of single ingredients and mixtures increased at higher protein content.

The particle size of LPC was clearly smaller than that of LF and LPI (LF < LPI). However, the mixtures showed increasing particle size at higher protein content (M3 > M2 > M1).

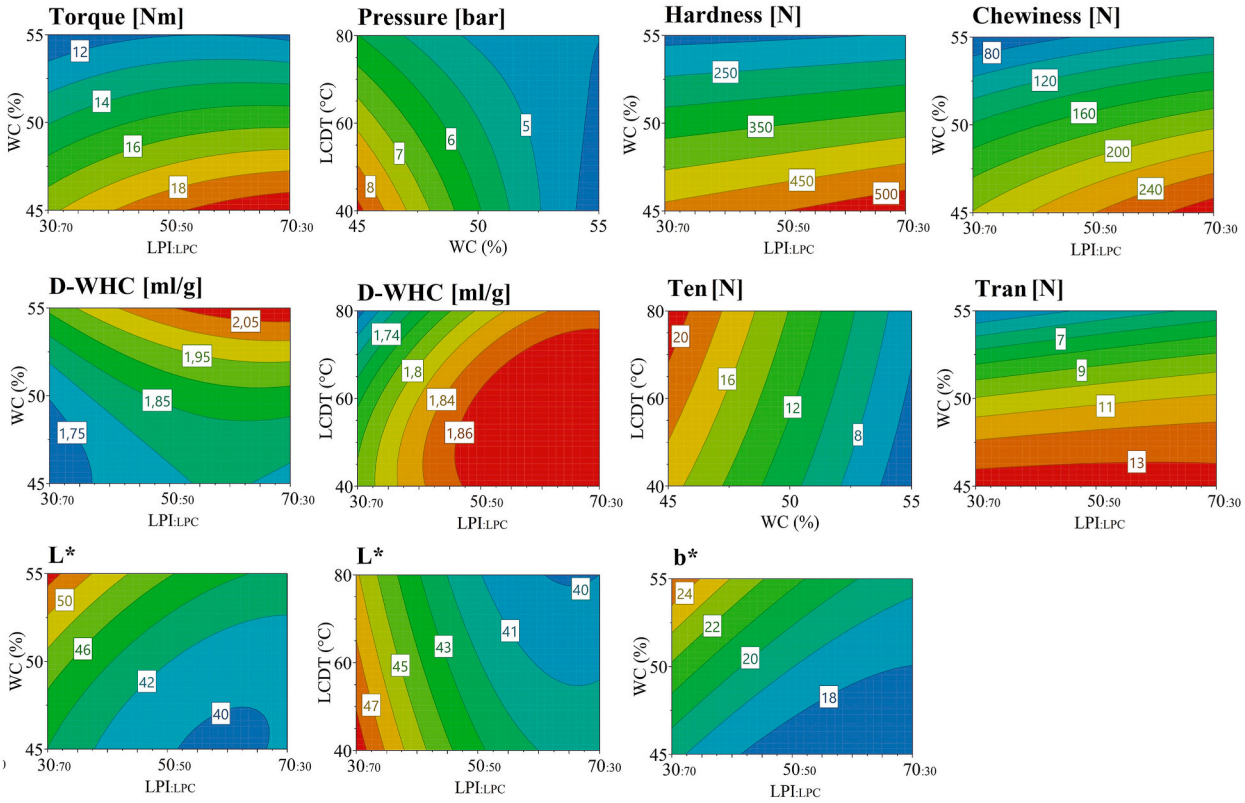

Fig. 1. Contour plots (2D) corresponding to process parameters, mechanical and physicochemical characteristics of TMAs in line with the MLR modelling (Table 2). Destructive water hydration capacity, *D-WHC*; Lightness, *L**; redness, *b**; tensile cutting strength, *Ten*; transverse cutting strength, *Tran*.

3.2. Effect of protein on TMA

A higher content of lupin protein (higher LPI:LPC blend ratio) increased torque (main effect) upon extrusion, whereas it seemed to have a negligible/minor effect on pressure (interaction effect; LPI:LPC blend ratio and LCDT) (Table 2; Fig. 1). Various studies [26,36, 37] have suggested a direct relationship between protein content and torque/pressure, generally associated with protein denaturation and texturization during extrusion.

A higher lupin protein content (higher LPI:LPC blend ratio) was directly proportional to hardness (calculated as shown in Equation (1)) and particularly chewiness (calculated as shown in Equation (3)) as shown in Table 2 and Fig. 1. The relationship between plant protein and sturdiness (defined as a robust structure characterized by high hardness or chewiness) was linked to the increasing presence of protein during extrusion [36]. Nevertheless, hardness and chewiness might be ascribed to higher protein–protein interactions at a higher LPI:LPC blend ratio.

The larger presence of hydrophilic groups could increase water bonding across a protein-rich continuous phase. As a result, a larger volume-mass fraction—containing bonded water and non-proteinaceous components such as carbohydrates—might be formed [28, 38]. Water and carbohydrates in a protein-rich phase may reduce the sturdiness of the overall structure [28]. In the present study, it is possible that the protein-rich phase showed hydrophobic traits, particularly at a higher lupin protein content (i.e., high LPI:LPC blend ratio). This could be a plausible explanation for the increase in the sturdiness in TMAs (Table 2; Fig. 1).

There was a direct impact of lupin protein content (higher LPI:LPC blend ratio) on the D-WHC of TMAs (calculated as shown in Equation (4); Table 2; Fig. 1). This seems to contravene the results shown by Ref. [39]; who demonstrated that a higher content of faba protein isolate substantially reduced water absorption capacity (technically the same as the ND-WHC) and, to a nonsignificant level, D-WHC. It is possible that, in the present study, the number of hydrogen bonds—between protein moieties (amine, amide, and hydroxyl groups) and water—increased at higher protein content. Interestingly, these changes were observed only in the D-WHC but not in the ND-WHC. The destructive nature of the method (i.e., D-WHC) may have increased the surface contact area between the protein and water, thus increasing the chances of bonding.

Regarding color, increasing protein content (higher LPI:LPC blend ratio) seemed to darken the TMAs (lower L*), and reduce their yellowness (lower b*) (Table 2; Fig. 1). These findings are in contrast to those of [40]; who showed that increasing soy protein isolate—in relation to hemp protein concentrate—resulted in lighter and yellower meat analogues. All the mixtures tested in the present study contained 30% (d.m.) native lupine flour. Apparently, mixtures with more dietary fiber/carbohydrates (low LPI:LPC blend ratio) were better at preserving lupin's light-yellow color compared to mixtures with less dietary fiber/carbohydrates (high LPI:PLC blend ratio). Further, the increasing protein content (high LPI:PLC blend ratio) in mixtures, which are rich in reducing sugars, may have encouraged non-enzymatic browning (Maillard reaction) during extrusion. The presence of phenolic compounds in lupin flour (e.g., flavonoids, flavonols, tartaric esters [19]; may also have intervened in color formation. It is plausible that the enzymatic oxidation of phenolic compounds occurred before compartment four (100 °C).

Color variation could also be associated with polyphenol–quinone conversion reactions with amino acids residues. If LPI were produced using the alkaline extraction before protein precipitation at their isoelectric points, phenolic compounds might have been oxidized to their quinones. According to Ref. [41]; these quinones could react with free NH_2 or thiol groups, producing dark pigmentation after condensation reactions. In this context [42], reported that flavonoids have a high affinity strength to γ-conglutin; a unique lupin protein. This finding seems to strengthen the link between darkening and the formation of protein–polyphenol conjugates and polymerization in TMAs.

3.3. Effect of processing conditions on TMA

During extrusion, the increase in water content decreased torque and pressure (Table 2; Fig. 1). The lubricating properties of water—on the mass undergoing extrusion—have been vastly reviewed by previous studies [43–45]. The present results also indicate that the increase of water content was associated with softer and less chewy structures in TMAs (Table 2). Hardness decreased by 50%, while chewiness decreased by almost 70% upon the increase in water content (from 45% to 55%; Fig. 1) [39]. observed comparable results during the extrusion of blends containing faba bean protein isolate and concentrate. In the present study, the increase in water content had a remarkable impact on hardness and chewiness, even compared to protein content (high LPI:LPC blend ratio).

Regarding water hydration, a higher water content led to an increase in the D-WHC (Table 2; Fig. 1). Initial increments of water content were associated with modest increase in the D-WHC up to an inflection point (around 50% water), after which the D-WHC rapidly increased. Interestingly, Kantanen et al. (2022) reported a similar effect of water content via non-destructive methods. In the present study, the addition of water may have increased the hydrogen bonding in the lupin protein as suggested by Ref. [46]. It is possible that water fostered molecular-level changes in the protein thereby increasing its hydration capacity, regardless of structural conditioning (powdering) prior to measurement. However, higher LCDT seemed to reduce the D-WHC. These changes were rather modest compared to those of water content. Thus, it is reasonable to think that temperature stimulated changes in the molecular configuration of proteins under specific processing conditions (low LPI:LPC blend ratio; Fig. 1).

The effect of water content on cutting strength was substantial. Tensile and transverse cutting strength was reduced at a higher water content. Additionally, the AI values around 1 (0.9–1.1) corresponded to samples with higher water content (Appendix A). This may indicate isotropy (or lack of anisotropy), as the cutting strength values were similar regardless of the cutting direction (tensile or transverse) [39]. It is possible that water may help open a tightly packed fibrous arrangement, thereby weakening the overall structure. In the present study, structural changes in the TMAs were strongly associated with a higher hydration capacity. These findings are consistent with those of [47]; who suggested a link between isotropy and the higher hydration capacity of fibrous meat analogues

(containing oat fiber concentrate and pea protein isolate).

Water content and LCDT presented statistically significant main effects and interactions on lightness (L*) and yellowness (b*). The higher the water content, the lighter and yellower the TMAs became. By contrast, a higher LCDT gave rise to a darker color. At a low LCDT, the increase in water content showed a substantial effect on the lightness of the TMAs. However, the effect of water progressively diminished as LCDT increased. Various studies [39,40,48] have reported the effects of temperature and water content on the darkening of extrudates.

3.4. PLSR modeling

PLSR allowed mapping and visualization of the cause-effect relationships between process parameters and the physicochemical characteristics of TMAs (Fig. 2). Among the process parameters, water content had the greatest effect, followed by the LPI:LPC blend ratio and LCDT. According to this model, a higher water content led to lighter (+L*), yellower (+b*), softer (i.e., low hardness, low cutting strength), and less chewy TMAs. The latter (hardness, cutting strength, and chewiness) also correlated with high pressure and torque. Further, a high LPI:LPC blend ratio seemed to increase water hydration (D-WHC and ND-WHC), reduce oil absorption (ND-OAC), and decrease lightness (-L*) and yellowness (-b*).

Using a similar modeling technique [47], observed that a high content of pea protein was linked to high water hydration and low oil absorption in TMAs. By contrast [39], observed a lower water hydration capacity in TMAs containing a high content of faba bean protein isolate [39]. also reported a substantially higher oil absorption capacity compared to those observed in the present study (Appendix A). In both studies [39,47], TMAs with high protein content showed a dark color compared to those with low protein content. In the present study, despite the high water content, the onset of Maillard reactions (non-enzymatic browning) may be fostered by the larger presence of amino acids (amino groups of lysine residues) and reducing sugars in the mass during extrusion. Besides, enzymatic browning (before the onset of protein denaturation) should not be entirely dismissed due to the presence of phenolic compounds in lupin mixtures, particularly in native lupin flour. The location of the LCDT at the center of the PLSR plot indicates that the LCDT cannot adequately explain the score variation under the current model. Similarly, the observed springiness (calculated as shown in Equation (2)) and redness (+a*) could not be satisfactorily explained.

3.5. Microtomography

Water content had an observable impact on the structure of the TMAs, as shown in Fig. 4A. Transitioning from 45% to 55% water content substantially reduced wall thickness. The drop was remarkably pronounced at a low LPI:LPC blend ratio (Fig. 4A). In line with

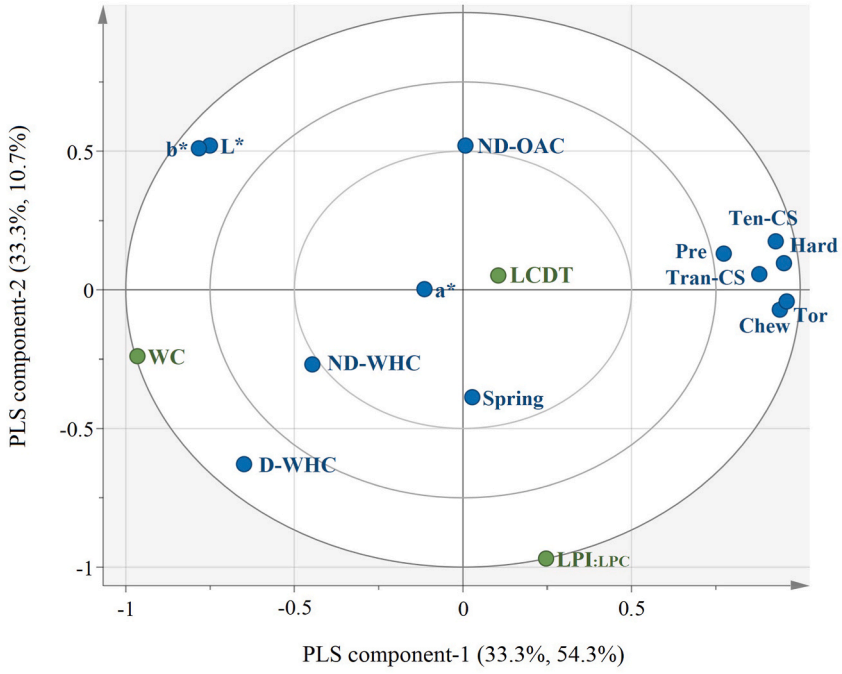

Fig. 2. PLSR plot describing the effect of independent extrusion variables (blend ratio between lupin protein isolate and concentrate, *LPI:LPC*; water content, *WC*; long cooling die temperature, *LCDT*) on process parameters (pressure, *Pre*; torque, *Tor*), mechanical (chewiness, *Chew*; hardness, *Hard*; springiness, *Spring*; tensile cutting strength, *Ten-CS*; transverse cutting strength, *Tran-CS*) and physicochemical (non-destructive water hydration capacity, *ND-WHC*; non-destructive oil absorption capacity, *ND-OAC*; destructive water hydration capacity, *D-WHC*; lightness, *L**; yellowness, *a**; redness, *b**) properties. The percentage variance in X and Y, explained by each PLSR component is shown next to the adjacent axes (X, Y).

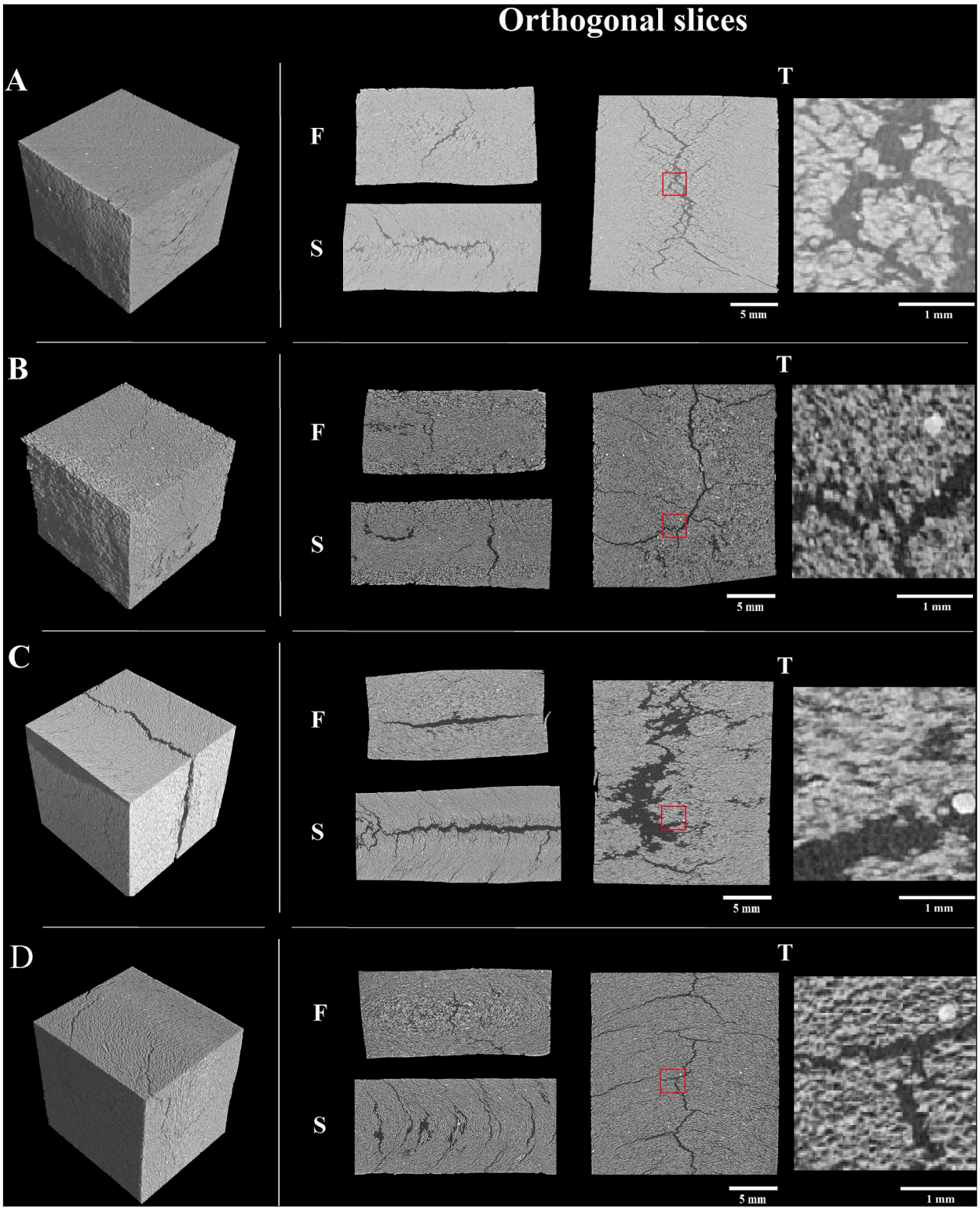

Fig. 3. Microtomography images of TMAs obtained at different blend ratios (*LPI:LPC*) and water contents (*WC*) as follows: A. 30:70 and 45%; B. 30:70 and 55%; C. 70:30 and 45%; D. 70:30 and 55%. Orthogonal slices from different view angles are shown: Front (*F*), Side (*S*) and Top (*T*).

this [39], reported a reduction in the wall thickness of TMAs (70% faba bean protein isolate) with increasing water content (from 60% to 65%). These changes in the LPI:LPC blend ratio had a minimal yet observable impact on the wall thickness of TMAs tested in the present study; however [39], found that wall thickness was considerably larger at a higher content of faba bean protein isolate.

TMAs containing more water (55%) showed—a larger probability of—smaller voids (Fig. 4B; <400 μm) than those containing less water (45%). Notably, TMAs containing a high LPI:LPC blend ratio (70:30) and low water content (45%) showed an abrupt increase in void thickness (Fig. 4B; <700 μm). As shown in Fig. 3, TMAs with low water content presented noticeable fractures along their geometric center. The formation of these fractures could be partially attributable to the physicochemical state of the mass during cooling. At this point, there is usually temperature/viscosity/velocity gradient (resembling Hagen–Poiseuille profile) between the inner and outer side of the mass, which affects water-protein phase separation (spinodal decomposition) and elongation [49]. The released of steam may depend—among other factors—on the capillarity and malleability of the mass upon phase separation. In the present study, water might have accumulated at the geometric center of the mass (as shown by the void distribution in the TMAs; Fig. 3A/3C). Apparently, high water content fostered a more homogenous water distribution across TMAs. This might explain the larger proportion of smaller voids in TMAs containing higher water content (Fig. 3B/3D; Fig. 4B).

Photographs of selected TMAs—same as those analyzed via microtomography—showed observable structural layering (Appendix E). Although TMAs with high water content seem to exhibit slightly better-defined layers than those with low water content, it is hard to link these observations to the microtomography results due to preconditioning factors (i.e., freeze-drying) and representativeness (e.g., size of the observed area). Additionally, TMAs with a high LPI:LPC blend ratio looked darker and less yellow. This is in line with the model-based results (MLR and PLSR) of the present study.

3.6. Fluorescence macroscopy

This method was developed for large-scale fluorescence analysis of extruded samples. As shown in Fig. 5, protein (red) and dietary fiber (black) were observed to be the largest components in the TMAs. Even though lipids, carbohydrates, and their corresponding complexes/aggregates were part of the system (white), they had minor presence in the TMAs, consistent with the chemical composition shown in Table 1. A noticeable difference between the center and side sections of the TMAs was observed (ΔmE was calculated as

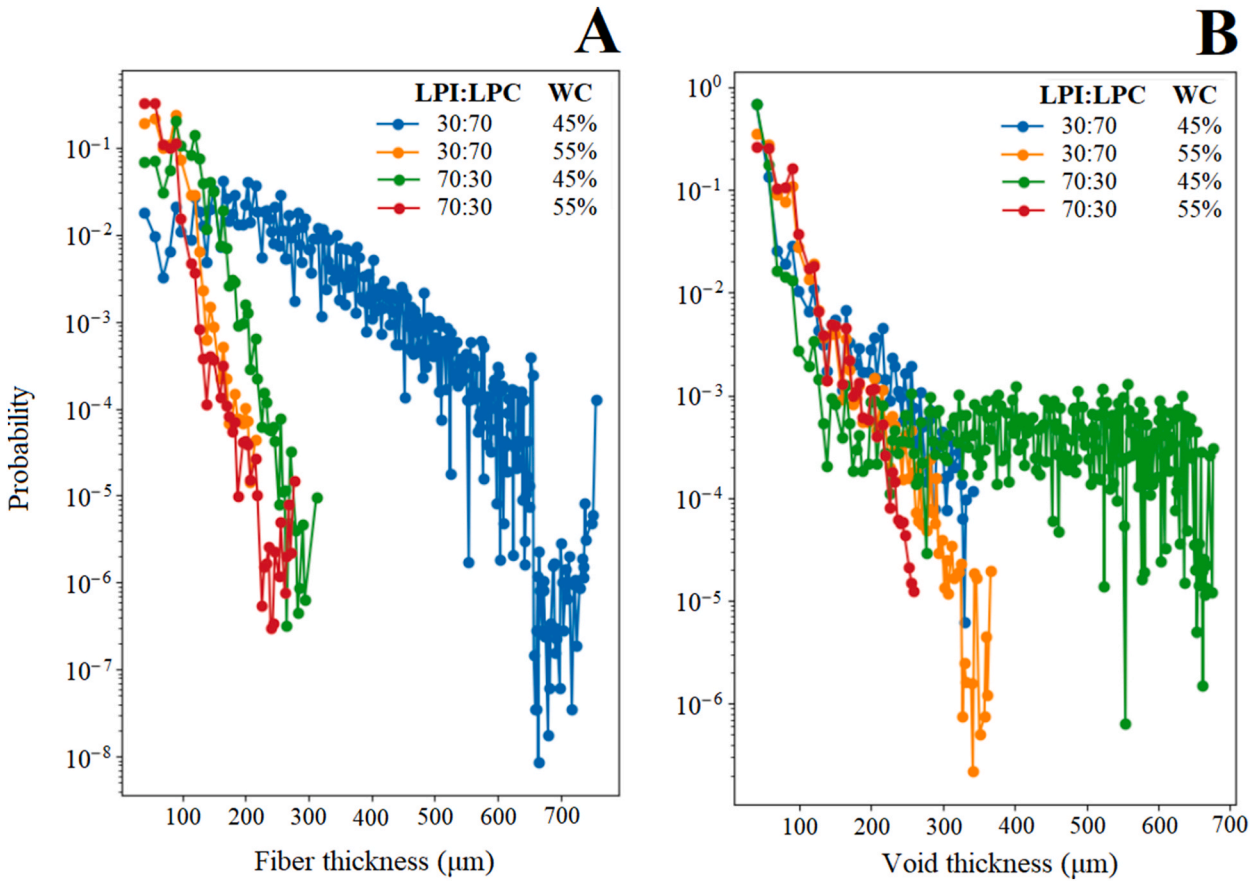

Fig. 4. Wall (A) and void thickness (B) probability distribution in TMAs obtained at two LPI:LPC blend ratios (30:70 and 70:30) and two water contents (45 and 55%).

shown in Equation (5); Fig. 5). Apparently, protein tended to concentrate at the geometrical center of the TMAs, particularly among those containing more LPI (LPI:LPC, 70:30; Fig. 5); the side section of these samples also presented observable fibrous structures.

The presence of dietary fiber in relation to protein was substantially higher in TMAs containing less LPI and obtained at 45% water content (LPI:LPC, 30:70; Fig. 5). The distinct presence of dietary fiber (black circular bodies) across this sample (LPI:LPC, 30:70; 45% water content; Fig. 5) coincided with the measurement of the thickest inner walls via microtomography (LPI:LPC, 30:70; 45% water content; Fig. 4A). Thus, it is reasonable to believe that dietary fiber was directly associated with the development of thicker walls (LPI:LPC, 30:70; 45% water content).

Based on color histograms (Fig. 5), the sample containing less LPI (LPI:LPC, 30:70) and obtained at 55% water content was compositionally the most homogenous (side vs. center; $\Delta mE = 7.74$). This also happened to be the sample with a remarkably low void thickness (Fig. 4A). By contrast, the sample containing more LPI (LPI:LPC, 70:30) appeared to be the most heterogeneous (side vs. center; $\Delta mE = 19.08$), yet it maintained its low void thickness (Fig. 4A). This supports the hypothesis that, at high availability, protein tends to accumulate at the geometric center of extrudates, with (apparently) minor consequences for void formation.

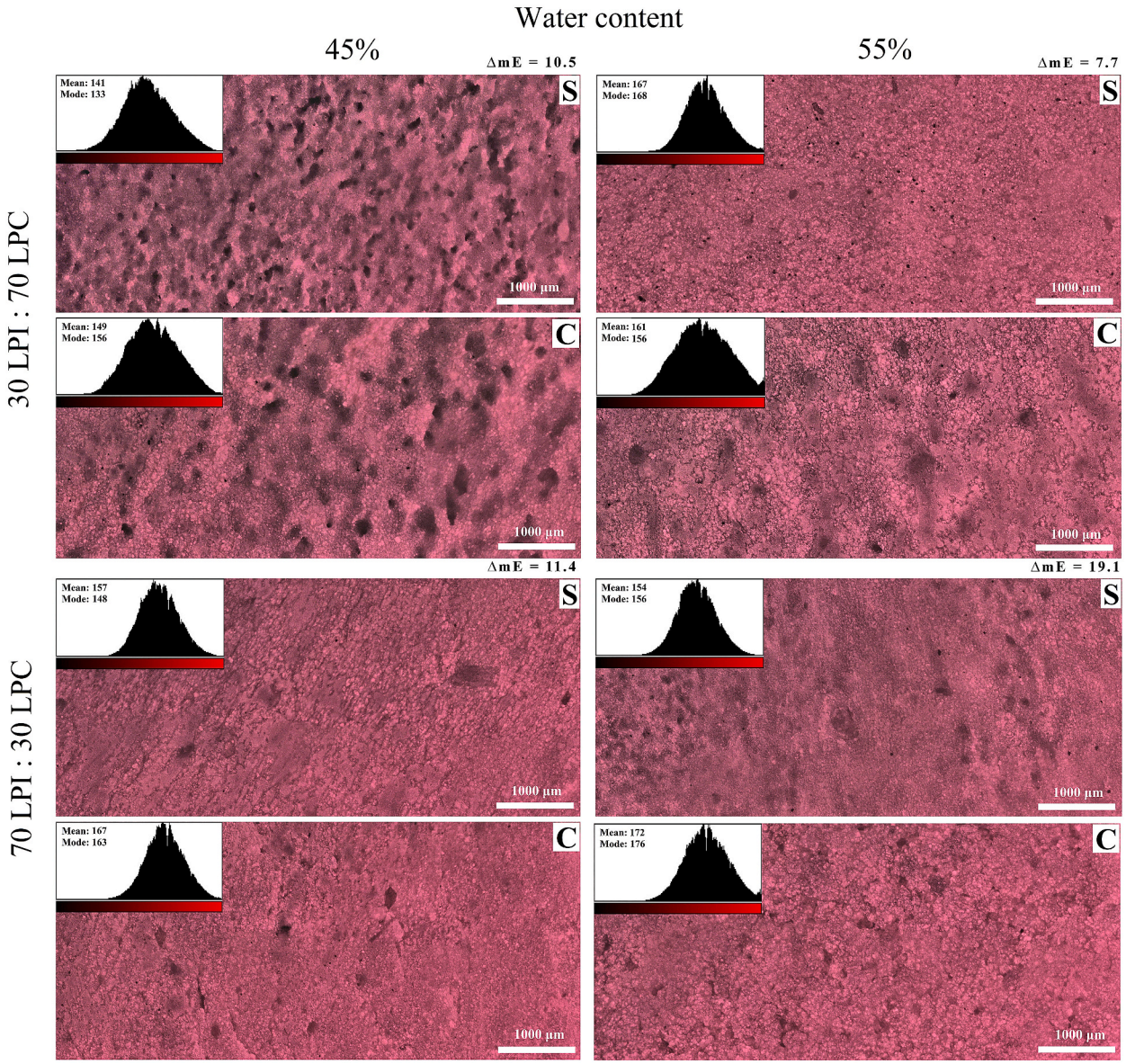

Fig. 5. Fluorescent composite imagery of TMAs containing two different LPI:LPC blend ratios (30:70 and 70:30) and processed at two different water contents (45% and 55%). Red, native or denatured protein; black, soluble/insoluble dietary fiber and carbohydrates; white, spectral overlap associated to the presence of neutral lipids (e.g., triglycerides). The red color histograms provide details (mean, mode) on the degree of blackness and redness of each image, and the overall color difference between center (C) and side (S) sections (ΔmE). (For interpretation of the references to color in this figure legend, the reader is referred to the Web version of this article.)

4. Conclusion

The present study showed that it is possible to obtain meat analogues by combining different blend ratios of lupin protein concentrate and isolate (70%) and a fixed fraction of native lupine flour (30%) under different processing conditions. High protein content was strongly linked to hardness and chewiness, while water content had the opposite effect on the mechanical properties of TMAs. Water content reduced cutting strength (tensile or transverse) and apparently had a negative impact on the formation of fibrous structures (e.g., AI close to 1). The hydration capacity of TMAs, either measured via destructive or non-destructive methods, increased with protein and water content. Regarding microtomography, the observed structures exhibited isotropic characteristics. The presence of small and homogeneously distributed voids was prevalent in TMAs with high water content. Fluorescence macroscopy revealed compositional differences between the center and side sections of the TMAs. Overall, increasing the LPI in the blend ratios led to detectable, yet not overwhelmingly different, technological changes (e.g., hardness, cutting strength) in the TMAs with side effects on darkening. TMAs with a low LPI presented technological characteristics that warrant further study. These findings strengthen the hypothesis that native flours can be used to obtain fibrous meat analogue if the protein content of the raw material is high enough, thus reducing over-reliance on protein ingredients. This study provides structural details that support process optimization and contributes to the body of knowledge on plant-based meat analogues from undervalued grain sources.

Author contribution statement

Ramos Diaz, J.M.: Conceived and designed the experiments; Performed the experiments; Analyzed and interpreted the data; Wrote the paper.

Oksanen, S., Kantanen, K., Edelmann, J.M, Suhonen, H.: Performed the experiments; Analyzed and interpreted the data.

Sontag-Strohm, T., Piironen, V., Jouppila, K.: Conceived and designed the experiments; Contributed reagents, materials, analysis tools or data.

Data availability statement

Data included in article/supp. material/referenced in article.

Declaration of competing interest

The authors declare that they have no known competing financial interests or personal relationships that could have appeared to influence the work reported in this paper.

Acknowledgements

This work has been funded by the Leg4Life project, supported by the Strategic Research Council at the Academy of Finland (grant number 327698).

Appendix A. Supplementary data

Supplementary data to this article can be found online at https://doi.org/10.1016/j.heliyon.2023.e20503.

References

[1] A.C. Hoek, P.A. Luning, P. Weijzen, W. Engels, F.J. Kok, C. de Graaf, Replacement of meat by meat substitutes. A survey on person- and product-related factors in consumer acceptance, Appetite 56 (2011) 662–673, https://doi.org/10.1016/j.appet.2011.02.001.

[2] S.S. Ho, A.S.F. Chuah, E.L.Q. Koh, L. Ong, V.Q.Y. Kwan, Understanding public willingness to pay more for plant-based meat: environmental and health consciousness as precursors to the Influence of Presumed Media Influence model, Environmental communication 16 (2022) 520–534, https://doi.org/10.1080/17524032.2022.2051576.

[3] Natural Resource Defense Council, Food Miles: How Far Your Food Travels Has Serious Consequences for Your Health and the Climate, Natural Resources Defense Council, New York, USA, 2007.

[4] M. Rapinski, R. Raymond, D. Davy, T. Herrmann, J.-P. Bedell, A. Ka, G. Odonne, L. Chanteloup, P.J. Lopez, E. Foulquier, E. Ferreira da Silva, N. El Deghel, G. Boëtsch, V. Coxam, F. Joliet, A.-M. Guihard-Costa, L. Tibere, J.-A. Nazare, P. Duboz, Local Food Systems under global influence: the case of food, health and environment in five socio-ecosystems 15 (2023) 2376, https://doi.org/10.3390/su15032376.

[5] W. Sobotka, M. Stanek, J. Bogusz, Evaluation of the nutritional value of yellow (Lupinus luteus) and blue lupine (Lupinus angustifolius) cultivars as protein sources in rats, Ann. Anim. Sci. 16 (2016) 197–207, https://doi.org/10.1515/aoas-2015-0062.

[6] M.R. Monteiro, A.B. Costa, S.F. Campos, M.R. Silva, C.O. Silva, H.S. Martino, M.P. Silvestre, Evaluation of the chemical composition, protein quality and digestibility of lupin (Lupinus albus and Lupinus angustifolius), O Mundo da Saúde 38 (2014) 251–259, https://doi.org/10.15343/0104-7809.20143803251259.

[7] S.A. Kaczmarek, M. Kasprowicz-Potocka, M. Hejdysz, Mikula, R. Rutkowski, The nutritional value of narrow-leafed lupin (Lupinus angustifolius) for broilers, J. Anim. Feed Sci. 23 (2014) 160–166, https://doi.org/10.1080/00071668.2011.639343.

[8] M.D. Fraser, R. Fychan, R. Jones, Comparative yield and chemical composition of two varieties of narrow-leafed lupin (Lupinus angustifolius) when harvested as whole-crop, moist grain and dry grain, Anim. Feed Sci. Technol. 120 (2005) 43–50, https://doi.org/10.1016/j.anifeedsci.2004.12.014.

[9] M. Duranti, A. Consonni, C. Magni, F. Sessa, A. Scarafoni, The major proteins of lupin seed: characterisation and molecular properties for use as functional and nutraceutical ingredients, Trends Food Sci. Technol. 19 (2008) 624–633, https://doi.org/10.1016/j.tifs.2008.07.002.

[10] H. Beyer, A.K. Schmalenberg, G. Jansen, H.U. Jürgens, R. Uptmoor, I. Broer, J. Huckauf, R. Dietrich, V. Michel, A. Zenk, F. Ordon, Evaluation of variability, heritability and environmental stability of seed quality and yield parameters of *L. angustifolius*, Field Crops Res. 174 (2015) 40–47, https://doi.org/10.1016/j.fcr.2014.12.009.

[11] K. Panasiewicz, Chemical composition of lupin (lupinus spp.) as influenced by variety and tillage system, Agriculture 12 (2022) 263, https://doi.org/10.3390/agriculture12020263.

[12] A. Sujak, A. Kotlarz, W. Strobel, Compositional and nutritional evaluation of several lupin seeds, Food Chem. 98 (2006) 711–719, https://doi.org/10.1016/j.foodchem.2005.06.036.

[13] M. Bähr, A. Fechner, K. Hasenkopf, S. Mittermaier, G. Jahreis, Chemical composition of dehulled seeds of selected lupin cultivars in comparison to pea and soya bean, LWT–Food Sci. Technol. 59 (2014) 587–590, https://doi.org/10.1016/j.lwt.2014.05.026.

[14] N. Musco, M.I. Cutrignelli, S. Calabro, R. Tudisco, F. Infascelli, R. Grazioli, V. Lo Presti, F. Gresta, B. Chiofalo, Comparison of nutritional and antinutritional traits among different species (*Lupinus albus L.*, *Lupinus luteus L.*, *Lupinus angustifolius L.*) and varieties of lupin seeds, J. Anim. Physiol. Anim. Nutr. 101 (2017) 1227–1241, https://doi.org/10.1111/jpn.12643.

[15] S.R. Thambiraj, M. Phillips, S.R. Koyyalamudi, N. Reddy, Antioxidant activities and characterisation of polysaccharides isolated from the seeds of Lupinus angustifolius, Ind. Crop. Prod. 2015 (2015) 950–956, https://doi.org/10.1016/j.indcrop.2015.06.028.

[16] S.R. Thambiraj, N. Reddy, M. Phillips, S.R. Koyyalamudi, Biological activities and characterization of polysaccharides from the three Australian Sweet Lupins, Int. J. Food Prop. 22 (2019) 522–535, https://doi.org/10.1080/10942912.2019.1588298.

[17] S.C. Smith, R. Choy, S.K. Johnson, R.S. Hall, C.M.A. Wildeboer-Veloo, G.W. Welling, Lupin kernel fiber consumption modifies fecal microbiota in healthy men as determined by rRNA gene fluorescent in situ hybridization, Eur. J. Nutr. 45 (2006) 335–341, https://doi.org/10.1007/s00394-006-0603-1.

[18] S.R. Thambiraj, M. Phillips, S.R. Koyyalamudi, N. Reddy, Yellow lupin (*Lupinus luteus* L.) polysaccharides: antioxidant, immunomodulatory and prebiotic activities and their structural characterization, Food Chem. 267 (2018) 319–328, https://doi.org/10.1016/j.foodchem.2018.02.111.

[19] B.D. Oomah, N. Tiger, M. Olson, P. Balasubramanian, Phenolics and antioxidative activities in narrow-leafed lupins (*Lupinus angustifolius* L.), Plant Foods Hum. Nutr. 61 (2006) 91–97, https://doi.org/10.1007/s11130-006-0021-9.

[20] A. Torres, J. Frias, C. Vidal-Valverde, Changes in chemical composition of lupin seeds (*Lupinus angustifolius*) after selective α-galactoside extraction, J. Sci. Food Agric. 85 (2005) 2468–2474, https://doi.org/10.1002/jsfa.2278.

[21] G. Boschin, A. Arnoldi, Legumes are valuable sources of tocopherols, Food Chem. 127 (2011) 1199–1203, https://doi.org/10.1016/j.foodchem.2011.01.124.

[22] S. Wang, S. Errington, H.H. Yap, Studies on Carotenoids from Lupin Seeds. Conference Paper at the 12th International Lupin Conference, 2008. Fremantle, Western Australia. ISBN 0-86476-153-8.

[23] A. Paraskevopoulou, E. Provatidou, D. Tsotsiou, V. Kiosseoglou, Dough rheology and baking performance of wheat flour-lupin protein isolate blends, Food Res. Int. 43 (2010) 1009–1016, https://doi.org/10.1016/j.foodres.2010.01.010.

[24] V. Jayasena, P.P.Y. Leung, S.M. Nasar-Abbas, Effect of lupin flour substitution on the quality and sensory acceptability of instant noodles, J. Food Qual. 33 (2010) 709–727, https://doi.org/10.1111/j.1745-4557.2010.00353.x.

[25] G. Doxastakis, I. Zafiriadis, M. Irakli, H. Marlani, C. Tananaki, Lupin, soya and triticale addition to wheat flour doughs and their effect on rheological properties, Food Chem. 77 (2002) 219–227, https://doi.org/10.1016/S0308-8146(01)00362-4.

[26] M. Palanisamy, K. Franke, R.G. Berger, V. Heinz, S. Töpfl, High moisture extrusion of lupin protein: influence of extrusion parameters on extruder responses and product properties, J. Sci. Food Agric. 99 (2019) 2175–2185, https://doi.org/10.1002/jsfa.9410.

[27] M. Palanisamy, S. Töpfl, R.G. Berger, C. Hertel, Physicochemical and nutritional properties of meat analogues based on Spirulina/lupin protein mixtures, European Food Research and Technology 245 (2019) 1889–1898, https://doi.org/10.1007/s00217-019-03298-w.

[28] J. Zhang, Q. Chen, D.L. Kaplan, Q. Wang, High-moisture extruded protein fiber formation toward plant-based meat substitutes applications: science, technology, and prospect, Trends Food Sci. Technol. 128 (2022) 202–2016, https://doi.org/10.1016/j.tifs.2022.08.008.

[29] M.Y. Dansby, A.C. Bovell-Benjamin, Physical properties and sixth graders' acceptance of an extruded ready-to-eat sweetpotato breakfast cereal, J. Food Sci. 68 (2003) 2607–2612, https://doi.org/10.1111/j.1365-2621.2003.tb07069.x.

[30] AACC American Association of Cereal Chemists, International Approved Methods of Analysis, eleventh ed., AACC International, St. Paul, Minnesota, 2010.

[31] C.T. Rueden, J. Schindelin, M.C. Hiner, B.E. DeZonia, A.E. Walter, E.T. Arena, K.W. Eliceiri, ImageJ2: ImageJ for the next generation of scientific image data, BMC Bioinf. 18 (2017) 529, https://doi.org/10.1186/s12859-017-1934-z.

[32] J. Schindelin, I. Arganda-Carreras, E. Frise, V. Kaynig, M. Longair, T. Pietzsch, S. Preibisch, C. Rueden, S. Saalfeld, B. Schmid, J.-Y. Tinevez, D.J. White, V. Hartenstein, K. Eliceiri, P. Tomancak, A. Cardona, Fiji - an Open Source platform for biological image analysis, Nat. Methods 9 (2012) 676–682, https://doi.org/10.1038/nmeth.2019.

[33] A. Buades, B. Coll, J.-M. Morel, Non-local means denoising Image Processing On Line 1 (2011) 208–212, https://doi.org/10.5201/ipol.2011.bcm_nlm.

[34] J. Darbon, A. Cunha, T. Chan, S. Osher, G. Jensen, Fast Nonlocal Filtering Applied to Electron Cryomicroscopy Proceeding Published in 5th IEEE International Symposium on Biomedical Imaging: from Nano to Macro. Paris, France, 2008, https://doi.org/10.1109/ISBI.2008.4541250.

[35] R.P. Dougherty, K.-H. Kunzelmann, Computing Local Thickness of 3D Structures with ImageJ Microscopy and Microanalysis, vol. 13, 2007, pp. 1678–1679, https://doi.org/10.1017/S1431927607074430.

[36] S. Lin, H.E. Huff, F. Hsieh, Texture and chemical characteristics of soy protein meat analog extruded at high moisture, J. Food Sci. 2 (2000) 264–269, https://doi.org/10.1111/j.1365-2621.2000.tb15991.x.

[37] S. Lin, H.E. Huff, F. Hsieh, Extrusion process parameters, sensory characteristics, and structural properties of a high moisture soy protein meat analog, J. Food Sci. 67 (2002), https://doi.org/10.1111/j.1365-2621.2002.tb09454.x, 2002.

[38] B.L. Dekkers, M.A. Emin, R.M. Boom, A. van der Goot, The phase properties of soy protein and wheat gluten in a blend for fibrous structure formation, Food Hydrocolloids 79 (2018) 273–281, https://doi.org/10.1016/j.foodhyd.2017.12.033.

[39] K. Kantanen, A. Oksanen, M. Edelmann, H. Suhonen, T. Sontag-Strohm, V. Piironen, J.M. Ramos-Diaz, K. Jouppila, Physical properties of extrudates with fibrous structures made of faba bean protein ingredients using high moisture extrusion, Foods 11 (2022) 1280, https://doi.org/10.3390/foods11091280.

[40] I. Zahari, F. Ferawati, A. Helstad, C. Ahlström, K. Östbring, M. Rayner, J.K. Purhagen, Development of high-moisture meat analogues with hemp and soy protein using extrusion cooking, Foods 9 (2020) 772, https://doi.org/10.3390/foods9060772.

[41] F. Shahidi, C.S. Dissanayaka, Phenolic-protein interactions: insight from in-silico analyses – a review, Food Production, Processing and Nutrition 5 (2023) 2, https://doi.org/10.1186/s43014-022-00121-0.

[42] J. Czubinski, K. Dwiecki, Molecular structure-affinity relationship of selected phenolic compounds for lupin seed γ-conglutin, Food Hydrocolloids 128 (2022), 107561, https://doi.org/10.1016/j.foodhyd.2022.107561.

[43] S.X. Liu, M. Peng, S. Tu, H. Li, L. Cai, X. Yu, Development of a new meat analog through twin-screw extrusion of defatted soy flour-lean pork blend, Food Sci. Technol. Int. 11 (2005) 463–470, https://doi.org/10.1177/1082013205060130.

[44] J.M. Ramos-Diaz, S. Kirjoranta, S. Tenitz, P.A. Penttilä, R. Serimaa, A.-M. Lampi, K. Jouppila, Use of amaranth, quinoa and kañiwa in extruded corn-based snacks, J. Cereal. Sci. (2015) 59–67, https://doi.org/10.1016/j.jcs.2013.04.003.

[45] J.M. Ramos-Diaz, L. Sundarrajan, S. Kariluoto, A.-M. Lampi, S. Tenitz, K. Jouppila, Partial least squares regression modelingof physical and chemical properties of corn-basedsnacks containing kañiwa and lupin, J. Food Process. Eng. 40 (2017), e12396, https://doi.org/10.1111/jfpe.12396.

[46] S. Yoshioki, Dynamics of a protein and water molecules surrounding the protein: hydrogen-bonding between vibrating water molecules and a fluctuating protein, J. Comput. Chem. 23 (2001) 402–413, https://doi.org/10.1002/jcc.1170.

[47] J.M. Ramos-Diaz, K. Kantanen, J.M. Edelmann, H. Suhonen, T. Sontag-Strohm, K. Jouppila, Piironen, Fibrous meat analogues containing oat fiber concentrate and pea protein isolate: mechanical and physicochemical characterization, Innovat. Food Sci. Emerg. Technol. 77 (2022), 102954, https://doi.org/10.1016/j.ifset.2022.102954.

[48] C. Do Carmo, S.H. Knutsen, G. Malizia, T. Dessev, A. Geny, H. Zobel, K.S. Myhrer, P. Varela, S. Sahlstrom, Meat analogues from a faba bean concentrate can be generated by high moisture extrusion, Future Foods 3 (2021), 100014, https://doi.org/10.1016/j.fufo.2021.100014.

[49] J.L. Sandoval-Murillo, R. Osen, S. Hiermaier, G. Ganzenmüller, Towards understanding the mechanism of fibrous texture formation during high-moisture extrusion of meat substitutes, J. Food Eng. 242 (2019) 8–20, https://doi.org/10.1016/j.jfoodeng.2018.08.009.